

Published in final edited form as:

*Bioorg Med Chem.* 2014 April 1; 22(7): 2188–2193. doi:10.1016/j.bmc.2014.02.018.

## Studies on the antiproliferative effects of tropolone derivatives in Jurkat T-lymphocyte cells

Sophia N. Ononye, Michael D. Van Heyst, Charles Giardina, Dennis L. Wright, and Amy C. Anderson

Department of Pharmaceutical Sciences, University of Connecticut, 69 N. Eagleville Rd., Storrs, CT 06269

### Abstract

Thujaplicins are tropolone-derived natural products with antiproliferative properties. We recently reported that certain tropolones potently and selectively target histone deacetylases (HDAC) and inhibit the growth of hematological cell lines. Here, we investigated the mechanisms by which these compounds exert their antiproliferative activity in comparison with the pan-selective HDAC inhibitor, vorinostat, using Jurkat T-cell leukemia cells. The tropolones appear to work through a mechanism distinct from vorinostat. These studies suggest that tropolone derivatives may serve as selective epigenetic modulators of hematological cells with potential applications as anti-leukemic or anti-inflammatory agents.

### Keywords

HDAC inhibitor; tropolone; natural product; vorinostat; leukemia

## 1. Introduction

The tropolone nucleus is a naturally occurring non-benzenoid aromatic characterized by the presence of an alpha-hydroxy tropone unit, a potential metal-directing moiety. This nucleus occurs in relatively simple natural products such as thujaplicins (Fig. 1) as well as more complex molecules such as colchicine. Many of these molecules, especially those with free tropolones (e.g. thujaplicins), have been known to have antibacterial, antifungal, and antiproliferative activity<sup>1-3</sup>. Despite the abundance of this class of natural products, there have been few attempts to utilize this scaffold as a lead pharmacophore in drug development. Moreover, there have been very limited efforts to determine the mechanism of action through which these compounds exert their antiproliferative activity. We have come to view the thujaplicins as “lead-like natural products” whereby the low molecular weight, ample sites for diversification and the presence of a strong metal-directing pharmacophore

© 2014 Elsevier Ltd. All rights reserved.

Correspondence to: Dennis L. Wright; Amy C. Anderson.

**Publisher's Disclaimer:** This is a PDF file of an unedited manuscript that has been accepted for publication. As a service to our customers we are providing this early version of the manuscript. The manuscript will undergo copyediting, typesetting, and review of the resulting proof before it is published in its final citable form. Please note that during the production process errors may be discovered which could affect the content, and all legal disclaimers that apply to the journal pertain.

suggest that potent and selective inhibitors of metalloenzymes could be developed from this scaffold. In order to fully develop this class, it is necessary to devise flexible and rapid synthetic approaches to analogs as well as gain a more detailed understanding of the molecular pharmacology.

In prior work, we explored the possibility of developing inhibitors of the zinc-dependent histone deacetylases (HDACs) starting with simple substituted tropolones. The HDAC family of enzymes comprises 18 isozymes, 11 of which are zinc-dependent, which catalyze the hydrolysis of an  $\epsilon$ -acetamido group of key lysine residues in histones and lead to increased expression levels of target genes<sup>4, 5</sup>. Currently, HDAC inhibitors (HDACi) have been clinically validated for the treatment of cutaneous T-cell lymphoma (CTCL) with the approval of two compounds, vorinostat and romidepsin. Both approved agents are considered pan-inhibitors as they display potent activity against most of the zinc-dependent, class I and II HDAC isoforms<sup>5, 6</sup>. It is appreciated that some of the untoward side effects observed with the pan-inhibitors would be limited if more selective, isozyme-specific agents were available<sup>7-9</sup>. Moreover, isozyme-selective HDAC inhibitors also offer the potential to produce specific epigenetic modulation in a non-cytotoxic manner, a feature that would be critical in treating disease states other than cancer, such as neurological or inflammatory disorders<sup>10-14</sup>.

Previously, we synthesized a small library of tropolones and found that substitution about the tropolone nucleus allows for the exploitation of key residue differences between HDAC isozymes and achieves good levels of selectivity, specifically for HDAC2 and HDAC8<sup>15</sup> (Figure 1). In addition, many of these derivatives show very specific antiproliferative activity against hematological lines ( $IC_{50} < 1 \mu M$ ) with little observed toxicity toward other cancer types or normal cells. This specific enzyme and cellular activity profile suggests that this class may be optimized to function as more specific anti-leukemic agents, T cell modulators or low-toxicity epigenetic modulators in other tissues. In order to gain deeper insight into the mechanisms by which they exert the antiproliferative effects and how those effects differ from pan-HDAC inhibitors, we investigated the cellular effects of two tropolones with the most potent antiproliferative activity on a hematological cell line (Figure 1: compounds **1** and **2**). As a negative control, we also include in our studies compound **4**, a tropolone with a methyl ether that has reduced metal coordination and HDAC inhibition. We demonstrate that the HDAC-inhibiting tropolones are growth inhibitory, but work through a mechanism that is distinct from the pan-HDAC inhibitor, vorinostat. Our work also suggests that the tropolones may be useful for the development of more specific HDAC inhibitors with distinctive pharmacological properties.

## 2. Results

As shown in previous work, several tropolone derivatives with HDAC inhibitory activity exhibit antiproliferative effects, especially toward hematological cell lines. As the pan-HDAC inhibitor, vorinostat, also displays significant activity against these cell lines, it was important to determine whether the tropolones and vorinostat share common modes of action or whether they inhibit cell growth through alternative mechanisms. Toward this goal,

we evaluated how tropolones and vorinostat affected patterns of histone acetylation, cell cycle arrest and apoptosis in the Jurkat cell line.

### 2.1. Tropolones show selective alteration of histone acetylation states

Exposure to pan-HDAC inhibitors, including vorinostat, results in accumulation of hyperacetylated histones, most notably at lysine 9 or 23 of histone H3 and lysine 12 of histone H4<sup>6, 16</sup>. We recently reported that Jurkat cells treated with tropolone derivatives exhibit H4K12Ac hyperacetylation at levels of ~6-fold over control cells<sup>15</sup>. In order to explore the specificity of histone modulation, we investigated the levels of H3K9Ac and H3K23Ac hyperacetylation in Jurkat cells following a 12h treatment with the HDAC inhibitors<sup>17</sup> (Table 1, corresponding histograms are shown in Supplemental Information Figure S1). While vorinostat increased acetylation 10-fold and 1.5-fold at histone H3K9 and H3K23, the tropolones had a more modest effect. Compound **1** induced a modest two-fold increase in histone H3K9 acetylation in the Jurkat cells and no tropolone showed increased histone H3K23 acetylation. Furthermore, in a similar vein, we previously reported that tropolones do not induce tubulin hyperacetylation, consistent with a lack of HDAC6 inhibition<sup>15</sup>, unlike pan-HDAC and HDAC6-selective inhibitors<sup>18</sup>. Taken together, these observations suggest that the isozyme selectivity of the tropolones produces unique patterns of hyperacetylation relative to pan-HDAC inhibitors such as vorinostat.

### 2.2. Overexpression of p21 may not be required for tropolone-mediated growth inhibition

Treatment of cells with HDAC inhibitors has been shown to induce gene expression changes. In related experiments, we observed that treatment of colon cancer cell lines with several tropolone derivatives enhanced the expression of a variety of genes but with a profile distinct from vorinostat<sup>19</sup>. As activation of the CDK inhibitor, p21<sup>CIP1/WAF1</sup><sup>5, 20</sup> is a hallmark of pan-HDAC inhibitors, we investigated whether the tropolones also activate p21 expression. To measure these effects, p21 protein expression in Jurkat cells was determined using flow cytometry after a 24h treatment with 10  $\mu$ M and 50  $\mu$ M concentrations of the tropolones and vorinostat and mRNA levels were quantified with qRT-PCR (Figure 2; accompanying histograms are in Figure S2, Supporting Information). After a 24h period, vorinostat treatment resulted in a three-fold increase in p21 protein levels as well as a 300-fold increase in mRNA levels. Although compound **1** showed a slight increase at the protein level there was no measurable increase at the mRNA level at either 10  $\mu$ M or 50  $\mu$ M treatments in Jurkat cells. These data suggest that p21 activation may not be a primary mechanism for tropolone-mediated growth inhibition in Jurkat cells.

### 2.3. Tropolones affect cell cycle progression and apoptosis of Jurkat cells

HDAC inhibitors of various structural classes have been shown to induce G1, S phase and/or G2/M arrest and concurrently disrupt mitotic progression in proliferating cells in normal and malignant tissues<sup>5-7</sup>. To investigate the mechanism by which the tropolones inhibit the growth of hematological cells, we performed cell cycle analyses at multiple time points using Jurkat cells (Table 2; corresponding histograms are shown in Supporting Information). Compounds **1** and **2** induced the appearance of sub-diploid cells (<G0/G1) at the 12h, 24h and 36h time points (Data for the 12h timepoint are shown in Table 2; data for 24h and 36h

are reported in Table S1). There was also a decrease in both the S-phase and G2-M phase cells following tropolone treatment at all three time-points, such that the majority of non-apoptotic cells were in G1. In contrast, treatment with the inactive tropolone methyl ether (compound **4**) resembled untreated controls. Conversely, vorinostat induced an increase in the population of subdiploid and G2-M cells at 12h. At 24h and 36h following vorinostat treatment, the percentage of apoptotic cells (<G0/G1) significantly increased to 48.90% and 60.80% respectively. Overall, the patterns of cell cycle arrest highlight the differences in activity between these tropolone compounds and classical pan-HDAC inhibitors.

#### 2.4. Tropolones induce apoptosis in a Caspase-8 independent manner

HDAC inhibitors, including vorinostat alone and/or in combination with other anticancer agents have been shown to induce apoptosis in a caspase-8 dependent manner in several malignant cells<sup>7,12,16,20,21</sup>. Thus, we used flow cytometric analysis to monitor the activation of caspase-8 by tropolones and vorinostat after a 24h treatment period in Jurkat cells. Whereas treatment with vorinostat resulted in a greater than 100-fold increase in caspase-8 activation, the tropolones exhibited no activation of caspase-8 relative to the untreated control (Table 3; Figure S4 Supporting Information). These data suggest that the extrinsic apoptotic pathway may not be involved in the initiation of apoptosis by tropolones and in fact that the mechanisms of apoptosis induced by vorinostat and the tropolones are different.

#### 2.5. Caspase-3 activation is involved in tropolone-mediated apoptosis

Based on the central role of caspase-3 in the execution of apoptosis, we conducted a time-dependent assessment of caspase-3/7 activation in Jurkat cells after treatment with HDAC inhibitor using an assay that correlates luminescence with caspase-3 activity<sup>22</sup>. Interestingly, after a 6h treatment, compound **1** and compound **2** activated a higher level of caspase-3 activity than vorinostat (data for 12h are found in Figure 3; data for 6h, 24h and 48h in Table S2; standard deviations in Table S3). At 12h, vorinostat activated a greater than 2-fold increase in caspase-3/7 activity when compared to the untreated control. The tropolones also activated an increase in caspase-3/7 activity at 12h, albeit at levels lower than vorinostat. For both the tropolones and vorinostat, caspase-3 activation dropped after 24h or 48h, potentially due to apoptotic cell breakdown and caspase leakage. This analysis indicates that caspase-3/7 activation by both the tropolones and vorinostat peaks at 12h, suggesting that caspase-3 activation may be one of the mechanisms for the execution of apoptosis in Jurkat cells that is common for both the tropolones and vorinostat.

#### 2.6. Evaluation of the ability of tropolones to enhance expression of perforin in Jurkat cells

Cytotoxic T lymphocytes (CTLs) and natural killer (NK) cells kill virally infected or tumor cells by secreting membrane-disrupting proteins known as perforin and a family of serine proteases known as granzymes that work together to induce apoptosis of the target cell<sup>23, 24</sup>. It has also been shown that Jurkat cells are themselves sensitive to the presence of exogenous granzyme and perforin<sup>25</sup> and that the depsipeptide FK228 (an HDAC inhibitor) increases the expression of perforin in T cells<sup>26</sup>. Therefore, we investigated the effect of the tropolones and vorinostat on the expression of perforin in Jurkat cells. A time-dependent analysis revealed a two-fold increase in the expression of perforin after a 48h treatment with

both vorinostat and compound **1** (Figure 4). The increased expression of perforin may be the result of enhanced cellular maturation linked to cell cycle arrest, and may also contribute to the downstream activation of caspase-3 through an autocrine or paracrine mechanism<sup>27, 28</sup>.

### 3. Discussion

Alteration of gene expression by small molecule inhibitors of histone deacetylases may offer a pathway to intervene in a variety of disease states. Currently, efforts to employ HDAC inhibitors focus primarily on cancer. The present set of clinically approved agents function broadly through inhibition of many different HDAC isoforms and as such, produce a fairly broad range of cellular effects. It is presumed that inhibitors with a more restrictive profile would activate a subset of target genes and would therefore have a more specific set of cellular effects. As such, more specific epigenetic modulators could potentially find application, especially in cases for which antiproliferative effects are not desired or greater tissue specificity is required.

Here we show that the tropolones exert their antiproliferative activity towards Jurkat cells in a manner that is distinct from the pan-HDAC inhibitor, vorinostat. While both the tropolones and vorinostat induce apoptosis in this cell line, it appears that the tropolones work through a more limited subset of cellular processes. Specifically, relative to vorinostat, the tropolones have a more modest effect on histone hyperacetylation and do not appear to induce the expression of p21. The patterns of cell cycle arrest are also clearly distinct. While vorinostat appears to induce an extrinsic pathway of apoptosis, the tropolones do not (although both increase caspase-3/7 activity). Both the tropolones and vorinostat also appear to enhance the expression of perforin, which may be linked to cell maturation and, potentially, activation of caspase-3. Overall, the more restrictive induction of apoptosis by the tropolones relative to the pan-HDAC inhibitors may allow for the development of more directed anti-leukemic agents. In addition, there are a number of inflammatory conditions that feature elevated levels of T cell proliferation that may benefit from more targeted HDAC inhibition, such as rheumatoid arthritis and multiple sclerosis<sup>29, 30</sup>. In this regard, the tropolone nucleus appears to be well-suited for generating HDAC inhibitors with distinct cellular effects and may lead to the generation of compounds with unique pharmacological benefits.

## 4. Experimental

### 4.1. Cell Culture

Jurkat cells were obtained from ATCC (Manassas, VA) and cultured in RPMI 1640 (ATCC) supplemented with 10% fetal bovine serum (FBS; Atlanta Biologicals, Lawrenceville, GA), 1% penicillin/streptomycin (PEN-STREP; Mediatech Inc., Manassas, VA) and 1% L-Glutamine (L-Glut; Mediatech Inc.). Vorinostat (SAHA) was obtained from Sigma Aldrich.

### 4.2. Analysis of histone modification and gene expression

Approximately  $1 \times 10^6$  logarithmic-phase Jurkat cells were treated with either a tropolone or vorinostat for the applicable treatment period. Control wells contained no HDACi. After pertinent exposure, cells were harvested, chilled on ice for 10 min, washed with PBS and

fixed with 4% (w/v) paraformaldehyde (PFA) for 20 min. Fixed cells were resuspended in 5% BSA/PBS and stored overnight at 4°C. Cells were permeabilized with PBS plus 0.5% (v/v) Triton-X-100, washed and blocked with 10% normal goat serum. Cells were then incubated with either H3K9Ac, H3K23Ac, perforin, or p21 using primary antibodies purchased from Cell Signaling Technology (Beverly, MA) at a 1:100 dilution in 5% BSA/PBS and a FITC conjugated secondary antibody (Millipore, Billerica, MA) at a 1:1000 dilution in 5% BSA/PBS. Following staining, cells were evaluated for fluorescence<sup>17</sup> using a Becton Dickinson (BD) FACSCalibur Flow Cytometer (San Jose, CA). Values for the geometric mean fluorescence intensities (GMFI), equivalent to the median cell population response, were obtained via analysis on the FlowJo Workstation (Treestar Inc., Ashland OR). Assay results were compared to published data when possible<sup>31,32</sup>

#### 4.3. Reverse-transcription PCR and quantitative real-time PCR analysis

Approximately  $5 \times 10^6$  Jurkat cells were treated with either a tropolone or vorinostat for 24h in 6-well culture plates (Corning Inc). Cells were then harvested and washed with ice-cold PBS. RNA was isolated using the Trizol reagent (Life Technologies) according to the instructions of the manufacturer. Two micrograms of extracted RNA was subjected to reverse transcription using the Applied Biosystems High Capacity cDNA kit according to the manufacturer's instructions. Following the PCR reaction, Taqman gene expression systems (Applied Biosystems) for p21 and beta-actin were prepared and added in triplicate to optical 96-well micro-titer plates (Applied Biosystems) containing one microliter of cDNA according to the instructions of the manufacturer. All cDNA samples were synthesized in parallel and qRT-PCR was performed in triplicate on an Applied Biosystem's 7500 Fast Real-Time PCR system and software. Relative mRNA expression for p21 was normalized to  $\beta$ -actin levels. p values <0.05 were considered to be significant. Standard deviation values are reported in Supplemental Information.

#### 4.4. Cell cycle Analyses

Approximately  $1 \times 10^6$  logarithmic-phase Jurkat cells were treated with either tropolones or vorinostat and incubated for 12h, 24h and 36h in 6-well culture plates (Corning Inc.). Control wells contained no HDACi. After pertinent exposure, cells were harvested, washed with cold phosphate-buffered saline (PBS). Cells were fixed with ice-cold 70% ethanol, incubated at 4°C for several hours and incubated overnight at -20°C. Fixed cells were stained with 50  $\mu$ g/mL of propidium iodide (Life Technologies) and 200  $\mu$ g/mL of DNA-free RNase A (Sigma Aldrich) and incubated in the dark for several minutes. Following staining, cells were analyzed for the distribution of DNA content using a BD FACSCalibur Flow Cytometer. Percentages of cell populations in each cell cycle phase were calculated based on DNA content histograms with the aid of the FlowJo Workstation. Assay results were compared to published reports on cell cycle analysis for the experimental control vorinostat<sup>21</sup>.

#### 4.5. Evaluation of induction of apoptosis

Approximately  $1 \times 10^6$  logarithmic-phase Jurkat cells were treated with either a tropolone or vorinostat for the pertinent time period in 6-well culture plates. Control wells contained no HDACi. After exposure, cells were harvested, washed with cold PBS, and resuspended in

Annexin-binding buffer (10 mM HEPES, 140 mM NaCl and 2.5 mM CaCl<sub>2</sub>, pH 7.4). Cells were stained with Annexin V conjugated with a fluorescein molecule (Life Technologies) according to the instructions of the manufacturer. Propidium iodide (PI; Life Technologies) was also added to the cell suspension as a dead cell indicator. Following staining, cells were analyzed for fluorescence using a BD FACSCalibur flow cytometer (Shi). Populations of cells were sorted with the aid of the FlowJo Workstation as follows: live cells [Annexin V (-), PI (-)]; early apoptotic cells [Annexin V (+), PI (-)]; late apoptotic/necrotic cells [Annexin V (+), PI (+)].

#### 4.6. Evaluation of Caspase-8 activation

Approximately  $1 \times 10^6$  logarithmic phase Jurkat cells were incubated in 6-well culture plates with 10  $\mu$ M of either a tropolone derivative or vorinostat for 24h. Untreated wells served as negative controls for the assay. Cells were harvested, washed with cold PBS and evaluated for caspase-8 activation via FACS analysis with the aid of a fluorescent inhibitor of caspases (FLICA) reagent (Vybrant FAM Caspase-8 assay kit, Life Technologies) according to the instructions of the manufacturer<sup>33</sup>. Assay data were collected with a BD FACSCalibur flow cytometer and analyzed with the FlowJo Workstation.

#### 4.7. Caspase-3/7 Analysis

Approximately  $2 \times 10^4$  logarithmic phase Jurkat cells were incubated in triplicate in 96-well culture plates with 10  $\mu$ M of either a tropolone or vorinostat for the applicable time period. Untreated wells served as experimental controls for the assay. Following treatment, Caspase-3/7 activity was measured in Jurkat cells using the luminescent Caspase-Glo 3/7 assay (Promega) according to the manufacturer's instructions. The luminescent signal generated from the assay is correlated with caspase-3/7 activity and luminescence was measured using a Veritas Microplate reader (Promega). p values <0.05 were considered to be significant. Standard deviation values are reported in Supplemental Information.

### Supplementary Material

Refer to Web version on PubMed Central for supplementary material.

### Acknowledgments

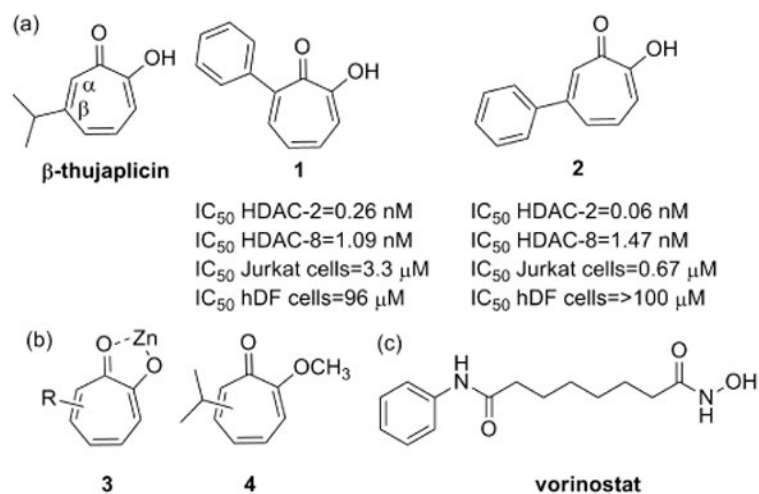
This work was supported by a grant from the National Institutes of Health (R21 CA162470).

### References

1. Liu S, Yamauchi H. *Biochem Biophys Res Commun.* 2006; 351:26–32. [PubMed: 17055455]
2. Liu S, Yamauchi H. *Cancer Lett.* 2009; 286:240–249. [PubMed: 19631451]
3. Oblak EZ, Bolstad E, Ononye S, Priestley N, Hadden MK, Wright D. *Org Biomol Chem.* 2012; 10:8597–8604. [PubMed: 23032214]
4. de Ruijter A, Gennip A, Caron H, Kemp S, van Kuilenburg A. *Biochem J.* 2003; 370:737–749. [PubMed: 12429021]
5. Marks P, Dokmanovic M. *Exp Opin Investig Drugs.* 2005; 14:1497–1511.
6. Dokmanovic M, Clarke C, Marks P. *Mol Cancer Res.* 2007; 5:981–989. [PubMed: 17951399]
7. Ononye S, Van Heyst M, Falcone E, Anderson A, Wright D. *Pharm Pat Analyst.* 2012; 1:207–221.

8. Balasubramanian S, Verner E, Buggy JJ. *Cancer Lett.* 2009; 280:211–221. [PubMed: 19289255]
9. Bieliauskas A, Pflum M. *Chem Soc Rev.* 2008; 37:1402–1413. [PubMed: 18568166]
10. Guan JS, Haggarty S, Giacometti E, Dannenberg JH, Joseph N, Gao J, Nieland T, Zhou Y, Wang X, Mazitschek R, Bradner J, DePinho R, Jaenisch R, Tsai LH. *Nature.* 2009; 459:55–60. [PubMed: 19424149]
11. Zhou Q, Dalgard C, Wynder C, Doughty M. *BMC Neuroscience.* 2011; 12:50. [PubMed: 21615950]
12. Lemoine M, Younes A. *Disc Med.* 2010; 10:462–470.
13. Adcock I, Tsaprouni L, Bhavsar P, Ito K. *Curr Opin Immunol.* 2007; 19:694–700. [PubMed: 17720468]
14. Ji M, Li G, Jia M, Zhu S, Gao D, Fan Y, Wu J, Yang J. *Inflammation.* 2013; 36:1453–1459. [PubMed: 23846716]
15. Ononye S, Van Heyst M, Oblak EZ, Zhou W, Ammar M, Anderson A, Wright D. *ACS Med Chem Lett.* 2013; 4:757–761.
16. Khan O, La Thangue N. *Immunol Cell Biol.* 2012; 90:85–94. [PubMed: 22124371]
17. Ronzoni S, Faretta M, Ballarini M, Pelicci P, Minucci S. *Cytometry Part A.* 2005; 66A:52–61.
18. Jose B, Okamura S, Kato T, Nishino N, Sumida Y, Yoshida M. *Bioorg Med Chem.* 2004; 12:1351–1356. [PubMed: 15018907]
19. Cao L, Kuratnik A, Xu W, Gibson J, Kolling F, Falcone E, Ammar M, Van Heyst M, Wright D, Nelson C, Giardina C. *Mol Carcinog.* 2013 in press.
20. Ouaiissi M, Giger U, Sielezneff I, Pirro N, Sastre B, Ouaiissi A. *J Biomed Biotechnol.* 2011; 2011:315939. [PubMed: 20981265]
21. Lobjois V, Frongia C, Jozan S, Truchet I, Valette A. *Eur J Cancer.* 2009; 45:2402–2411. [PubMed: 19553104]
22. Porter A, Janicke R. *Cell Death Differ.* 1999; 6:99–104. [PubMed: 10200555]
23. Armeanu S, Bitzer M, Lauer U, Venturelli S, Pathil A, Krusch M, Kaiser S, Jobst J, Smirnow I, Wagner A, Steinle A, Salih H. *Cancer Res.* 2005; 65:6321–6329. [PubMed: 16024634]
24. Trapani J, Smyth M. *Nat Rev Immunol.* 2002; 2:735–747. [PubMed: 12360212]
25. Wagner C, Iking-Konert C, Deneffle B, Stegmaier S, Hug F, Hansch GM. *Blood.* 2004; 103:1099–1104. [PubMed: 14512315]
26. Murakami T, Sato A, Chun N, Hara M, Naito Y, Kobayashi Y, Kano Y, Ohtsuki M, Furukawa Y, Kobayashi E. *J Invest Dermatol.* 2008; 128:1506–1516. [PubMed: 18185535]
27. Kagi, Vignaux F, Ledermann B, Burki K, Depraetere V, Nagata S, Hengartner H, Golstein P. *Science.* 1994; 265:528–530. [PubMed: 7518614]
28. Palmer D, Balasubramanian S, H Ki, Wrzesinski C, Yu Z, Farid S, Theoret M, Hwang L, Klebanoff C, Gattinoni L, Goldstein A, Yang J, Restifo N. *J Immunol.* 2004; 173:7209–7216. [PubMed: 15585842]
29. Hafler D, Weiner H. *Immunol Rev.* 1987; 100:307–332. [PubMed: 3326824]
30. Tristano A. *Int Immunopharmacol.* 2009; 9:1–9. [PubMed: 18848912]
31. Almenara J, Rosato R, Grant S. *Leukemia.* 2002; 16:1331–1343. [PubMed: 12094258]
32. Wozniak M, Villeundas R, Bischoff J, Aparicio C, Martinez L, de La Cueva P, Rodriguez M, Herreros B, Martin-Perez D, Longo M, Herrera M, Piris M, Ortiz-Romero P. *Haematologica.* 2010; 95:613–621. [PubMed: 20133897]
33. Smolewski P, Grabarek J, Halicka H, Darzynkiewicz Z. *J Immunol Methods.* 2002; 265:111–121. [PubMed: 12072182]



**Figure 1.**

a) Structures of the natural product  $\beta$ -thujaplicin and two synthetic tropolone derivatives with anti-proliferative activity, (b) tropolone nucleus interacting with a divalent zinc ion and an inactive derivative (c) Structure of the hydroxamate pan-HDAC inhibitor vorinostat

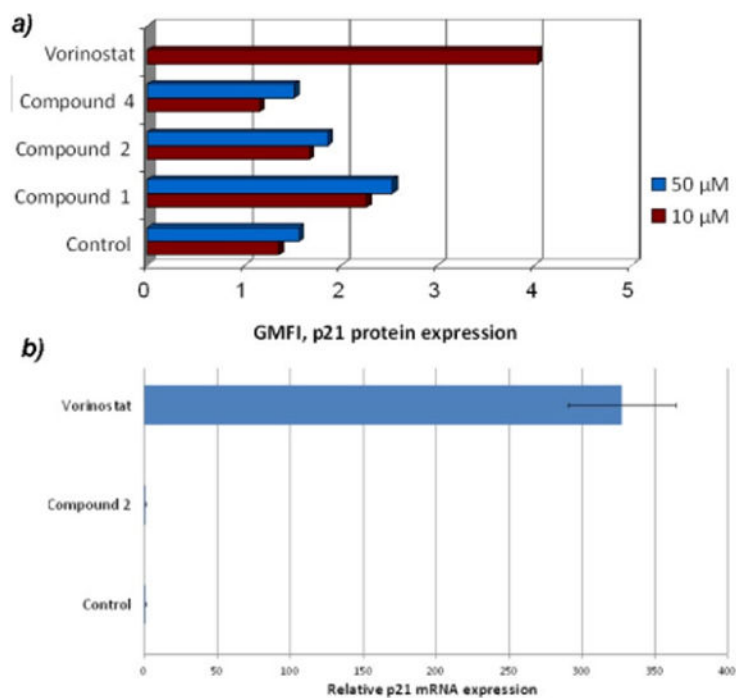


**Figure 2.**

p21 protein expression (a) and mRNA (b) after treatment of Jurkat cells at two concentrations (10  $\mu$ M and 50  $\mu$ M). Vorinostat treatment was performed with only 10  $\mu$ M owing to cytotoxicity at higher concentrations.

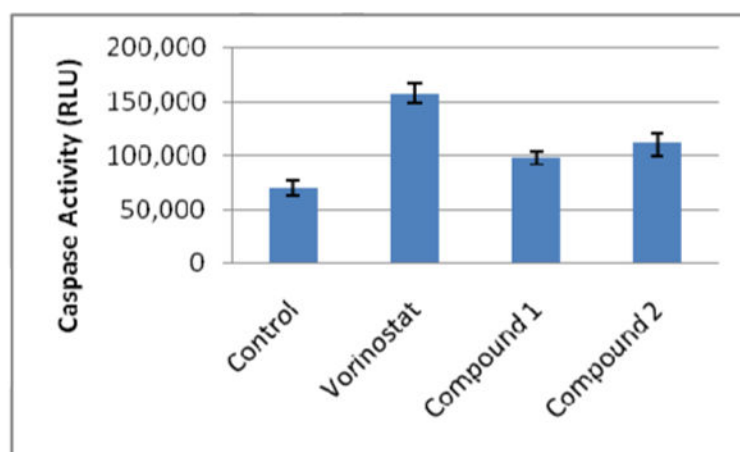


**Figure 3.**

Evaluation of Caspase-3/7 activation after a 12h treatment with 10  $\mu$ M HDACi.

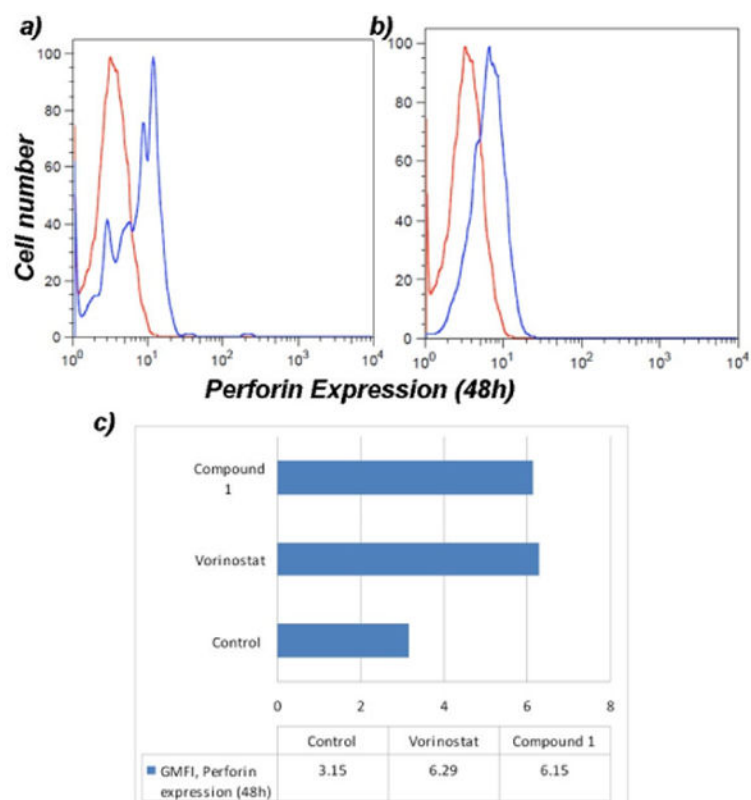


**Figure 4.**

Evaluation of the expression of perforin in Jurkat cells after a 48h treatment with a) vorinostat and b) compound **1**. Histograms represent the untreated control (red) superimposed with the HDACi treatment (blue) for comparative analysis.

Table 1

Histone hyperacetylation patterns (GMFI values<sup>a</sup>)

Trtmt	Cntl	Vor.	1	2	4
H3K9Ac	5.91	61.70	13.70	2.12	3.23
H3K23Ac	20.20	36.90	24.60	24.00	17.80

<sup>a</sup> GMFI: geometric mean fluorescence intensity is equivalent to the median population on a logarithmic scale

**Table 2**  
**Time-dependent analysis of the antiproliferative effects of tropolones on cell cycle progression as measured via flow cytometer analysis in Jurkat cells after a 12h treatment**

Trtmt	12h			
	%<G0/G1	%G1	%S	%G2-M
Control	4.16	65.0	19.5	10.0
Vor.	20.4	25.9	31.6	19.7
Cmpd 1	22.3	64.3	11.1	1.39
Cmpd 2	16.3	71.5	10.2	1.25
Cmpd 4	3.14	68.4	17.5	9.52

**Table 3**  
**Evaluation of Caspase 8 activation in Jurkat cells after a 24h treatment with 10  $\mu$ M HDACi**

Treatment	% Intact cells	%Caspase-8 responsive cells
Control	99.30	0.32
Vorinostat	62.60	35.90
Cmpd 1	98.90	0.43
Cmpd 2	99.40	0.40